analytical chemistry

Article

Cite This: Anal. Chem. 2019, 91, 7487−7494

pubs.acs.org/ac

Biosample Concentration Using Microscale Forward Osmosis with Electrochemical Monitoring

Martin K. Kimani,[†] Rachel Loo,[†] and Edgar D. Goluch*[,†,‡]

[†]Department of Chemical Engineering, Northeastern University, Boston, Massachusetts 02115, United States

[‡]Department of Bioengineering, Biology, Civil & Environmental Engineering, Northeastern University, Boston, Massachusetts 02115, United States

Supporting Information

ABSTRACT: We report the design and operation of an integrated microfluidics system that uses cellulose ester dialysis membranes coupled with disposable carbon and copper electrodes for monitoring and concentration of microliter scale biofluid samples. Dialysis membranes are typically used for buffer exchange, but in this work, membranes with 100−500 Da MWCO were evaluated for feasibility in concentrating small volume samples. This is an alternative to the use of centrifugation, ultrafiltration, and evaporative methods, where quantitative inline monitoring of sample concentration is challenging. The impact of draw solution used, osmotic concentration gradient, pH, and temperature were studied for the optimized concentration of bodily fluids. A system using sucrose in the draw solution generated the best results, with water removal rates of 0.023 mL min^{-1}. PBS, urine, and saliva samples were concentrated up to 20-fold (PBS), 15-fold (urine), and 5-fold (saliva) in less than 3 h. The osmotic system further showed a 5-fold increase in the electrochemical signal for detecting pyocyanin, a biomarker for early diagnostics of the *Pseudomonas aeruginosa* pathogen in urine and saliva samples. Overall, the osmotic system can be easily integrated with point of care diagnostic systems for low cost improvement in signal amplification and limit of detection.

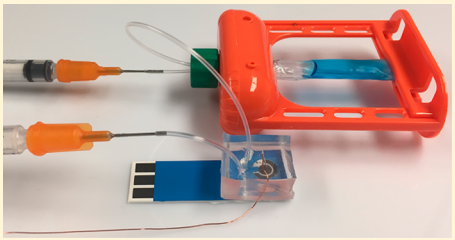

Conventional biomarker detection in bodily fluids involves the use of HPLC-MS,[1−4] capillary electrophoresis,[5−7] nuclear magnetic resonance techniques,[8−10] molecular imaging using positron-emission tomography (PET),[11] or PCR coupled with ELISA-based methods.[12−14] These methods are limited to laboratory use because they require sophisticated, costly equipment; are labor intensive; or require relatively more involved biosample preparation techniques.[15−17] In vitro diagnostic point of care testing (IVDPOCT) methods are becoming suitable alternatives as they provide low cost, ease of use, multiplexed, and immediate sample analysis by minimizing sample preparation.[18−23] On-going initiatives in developing point of care methods are improving detection limits and selectivity to rival results acquired with conventional laboratory methods.[21,24]

The design of IVDPOCT techniques requires special attention to both the limit of detection (LOD) and ability to use small sample volumes for analysis. Biomarkers found in bodily fluids are often in the subfemtomolar to millimolar range with acquired sample volumes in the milliliter to microliter range, so testing a microliter or less can result in minimal target molecules in the sample.[21,25] To improve LOD, some IVDPOCT approaches integrate PCR amplification with ELISA-based detection.[26] Dielectrophoresis, microfluidic chromatography, magnetic, and membrane separation are other methods that concentrate target biomarkers that can be coupled with sensors to improve the LOD in point of care systems.[27−29] Alternatively, detection surface area and geometry are being optimized using nano- and microstructures to improve LOD in affinity- and electrochemical-based detection systems.[30−32]

Sample concentration by volume reduction prior to analysis is a more convenient method for improving LOD in IVD-POCT systems, and it can also supplement conventional biomarker detection platforms.[33−35] Existing concentration methods in the microliter range use centrifugation for separating target pathogens and mammalian cells from the supernatant.[36,37] The cell pellet is subsequently reconstituted in the desired volume to acquire a more concentrated cell sample. For viruses, proteins, nucleic acids, and other small molecule biomarkers, centrifugation using molecular weight cutoff (MWCO) membrane is employed for reducing water volume in the sample, thereby concentrating the biomarkers.[33] Conventional centrifugation systems provide water removal rates of 0.33−1.07 mL min^{-1} when operated at temperatures between 45 and 100 °C. These systems use vacuum and increased temperatures during centrifugation for enhanced water evaporation from the desired sample.[38,39]

The disadvantage of these conventional sample concentration methods is the requirement of secondary and tertiary equipment, using centrifuges with pressure, temperature, and gas flow control that limit portability and integration with

Received: May 7, 2019
Accepted: May 9, 2019
Published: May 9, 2019

DOI: 10.1021/acs.analchem.9b02163
Anal. Chem. 2019, 91, 7487−7494

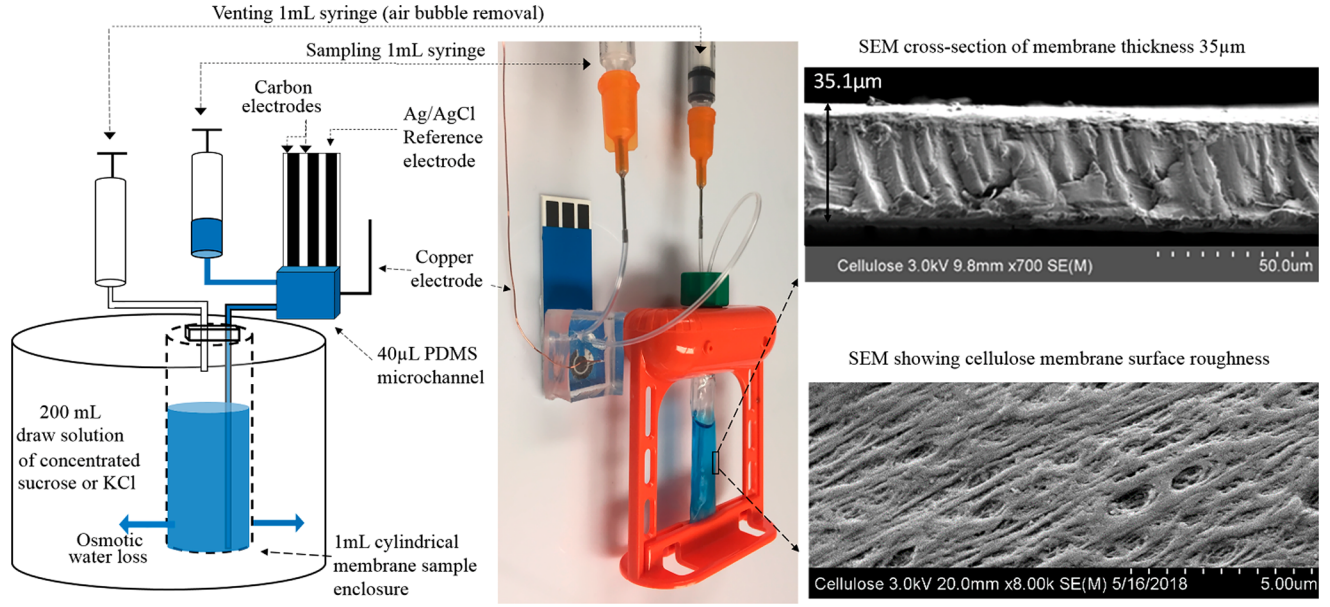

Figure 1. (Left) Schematic and photograph of a microfluidic concentration system with integrated monitoring of concentration and redox molecules using carbon and copper electrodes. (Right) Scanning electron micrographs of the cellulose ester dialysis membrane used for forward osmosis.

IVDPOCT systems.[28,34,40] Additionally, the quantitative determination of sample concentration is based on the initial and final liquid volume or mass measurements as reported by the operator, which propagate error in the accuracy of results.

A precise measurement of sample concentration with limited secondary equipment is desirable for cost-effective improvement of the LOD. As summarized below, there have been several designs for concentrating bodily fluid samples using evaporative concentration microfluidic systems,[34,40−42] paper-based evaporation with semipermeable membranes,[28] and using water adsorptive polymers.[43] Our proposed system introduces forward osmosis integrated with impedance measurements for the quantitative concentration of samples.

Evaporative Microfluidic Concentrators. Walker and Beebe presented the feasibility of using evaporative-based volume reduction by concentrating fluorescent spheres in a PDMS flow system.[44] Timmer,[42] Sharma,[41] and Tseng[35] reported evaporative microfluidic systems utilizing hydrophobic membranes with gas flow for convective water loss from a sample. These systems were capable of removing 0.006, 0.8, and 0.4 mL min^{-1} of water, respectively, when operated at temperatures around 40 °C.[35] Ho adopted the evaporation microfluidic device with integrated dialysis for blood concentration to detect HIV viral particles. This system performed dialysis to enable protein stabilization by depleting saline ions through a semi permeable membrane using a peristaltic pump for continuous flow. Samples were concentrated from 800 down to 100 μL in 30 min, yielding a water removal rate of 0.023 mL min^{-1}.[34] These evaporative microfluidic systems eliminate centrifugation and miniaturize volume reduction processes. However, they require secondary equipment for gas flow control and pumping or pressure driven flow to force the sample through the microfluidic system. Additionally, inline sample monitoring is not present; hence, the final concentrated sample has to be recovered from the system in order to determine extent of concentration.

Paper-Based Concentrators. Paper-based devices utilize capillary action for liquid flow. Wong designed a paper-based concentration device for tuberculosis diagnosis by detecting lipoarabinomannan (LAM) in urine.[40] The device used a resistive heater for the rapid evaporation of liquid from urine at 220 °C on a paper substrate. The group showed that the temperature did not compromise the subsequent immune-detection of LAM, and they were able to acquire overall water removal rates of 0.030 mL min^{-1} to achieve a 20-fold concentration in 20 min.[40] Tang designed another version of a paper-based lateral flow assay (LFA) that was coupled with a semipermeable membrane to improve the sensitivity of the LFA technique for detecting HIV viral particles.[28] In this design, PEG 8000 was used as a dialysate to draw water and saline ions through a semipermeable membrane of 3.5 kDa MWCO size to improve the LOD of the assay. The water removal rates in this system were not studied, but the dialysis led to a 2−4-fold increase in the optical density readout for the assay after 20 min.[28] These paper-based concentration methods can be integrated with other paper-based sensors, but they are more difficult to integrate into nonpaper-based IVDPOCT systems. Once the water volume has been removed, the sample contents may not be recoverable as they are embedded in the paper.

Water Adsorptive Polymer Concentrators. Alternative nonpaper-based concentration systems involve using water absorptive materials. Xie reported the use of superabsorbent polymer (SAP) beads for concentrating microorganisms in milliliter volume water samples.[43] The SAP beads were able to reduce 10 mL of water down to 1 mL in 50 min. The process required removal of the sample and placement into a new bed of SAP beads every 10 min to maintain an optimal water removal rate of 0.18 mL min^{-1}. They report that some molecules can diffuse into the beads during water absorption, but microorganisms remain in the sample.[43] This method eliminates the use of secondary equipment and is ideal for concentrating microorganisms, but it is more difficult to implement for biomarkers that are likely absorbed by the polymer beads.

DOI: 10.1021/acs.analchem.9b02163
Anal. Chem. 2019, 91, 7487−7494

Osmotic Concentration. We have recently reported an initial osmotic system for bacterial concentration and detection in growth medium using polyethylene glycol as the draw solute.[45] In the present study, we utilize sugar and salt as draw solutes, while focusing on membrane performance and characterization for integration with point of care analysis of urine and saliva. We designed the osmosis-driven microfluidic system shown in Figure 1 to concentrate bodily fluid samples up to 20-fold without secondary equipment. Once the sample is concentrated to the desired level using this design, it is easily recovered for further analysis. Forward osmosis is regularly used alongside reverse osmosis in drinking water recovery systems.[46] However, the current focus is on large scale processes, where dozens of liters are processed per hour, and special grade membranes are fabricated for optimal salt rejection.[47,48]

Unlike the water purification application, our design extracts water from bodily fluid samples thereby concentrating the biomarker of interest. We adapted the analysis from the large-scale system to characterize the performance of our device. The governing relationships for water flux through an active layer osmotic membrane are shown in eqs 1−4.

The driving force for water flux is due to the solute concentration difference across the membrane, which is quantified using osmotic pressure. Equation 1 defines the osmotic pressure (Π, pascals) through the Van't Hoff equation, where n is the number of moles of species formed when solute dissociates in solution, c (g/L) is the solute concentration, MW (g/mol) is the molecular weight of solute, R is the ideal gas constant, and T (K) is the absolute temperature.[49] Equation 2 defines the water flux (J_w, $m^3\ m^{-2}\ s^{-1}$ or $m\ s^{-1}$) across a membrane and relates it to the dimensionless osmotic reflection coefficient (σ), which correlates the ability of the solute to permeate through the membrane and is considered 1 for systems with minimal solute permeability, the water permeability coefficient (K, $m^3\ m^{-2}\ s^{-1}\ Pa^{-1}$ or $m\ s^{-1}\ Pa^{-1}$), and the difference between the osmotic pressures across the membrane ($\Delta\Pi$, pascals).[50] Equation 3 is derived from Fick's law of diffusion to describe the reverse solute flux rate (J_s, mol $m^{-2}\ s^{-1}$). It is the ratio between the solute concentration difference across the membrane (ΔC_s, $molm^{-3}$), the effective solute diffusion coefficient (D_e, $m^2\ s^{-1}$), and the membrane thickness (t, m). Finally the membrane design parameters for tortuosity (τ) and porosity (ε) are defined in eq 4 by correlating the effective solute diffusion coefficient (D_e, $m^2\ s^{-1}$) to the solute diffusion coefficient in free solution (D_s, $m^2\ s^{-1}$).[50,51] These correlations show that water flux is maximized when osmotic pressure across the membrane is high, and the solute diffusion through the membrane can be minimized by utilizing a membrane that has a small ratio of porosity to tortuosity.

$$\Pi = n\left(\frac{c}{\mathrm{MW}}\right)RT \tag{1}$$

$$J_w = \sigma K \Delta\Pi \tag{2}$$

$$J_s = D_e\frac{\Delta C_s}{t} \tag{3}$$

$$D_e = D_s\frac{\varepsilon}{\tau} \tag{4}$$

EXPERIMENTAL SECTION

Materials. Specialized forward osmosis membranes for small volume processes are not readily available, as forward osmosis processes are typically employed in large-volume industrial environments for water recovery. Therefore, commercially available dialysis grade membranes were used for the proof-of-concept. Cellulose ester membranes with 100−500 Da MWCO sizes were therefore sourced from Spectrum Laboratories (part F235061). Cellulose ester membranes are widely used in forward osmosis and dialysis membrane separations due to their high water permeability, low reverse solute rejection, and good chemical compatibility properties.[52,53] Figure 1 shows the membrane and scanning electron microscopy (SEM) images of the cross sectional thickness (35 μm) and surface roughness of the membrane. A more detailed overview of the device assembly is provided in the Supporting Information in Sections S1 and S2 and in Figure S1.

Electrochemical measurements were carried out using disposable, screen-printed electrode sensors made by Zensor, and purchased from CH Instruments (part TE100), that consist of carbon working (3 mm diameter) and counter electrodes and a silver/silver-chloride (Ag/AgCl) reference. Copper electrodes were fabricated in-house using copper removed from an Ethernet cable. Voltammetric electrochemical measurements were performed using a potentiostat from CH Instruments (part CHI 1040C). Impedance spectroscopy measurements were performed using an electrochemical workstation supplied by Zahner-Electrik (part IM6ex). Reagent grade chemicals were sourced from Fisher Scientific and included sodium chloride (CAS 7647-14-5), potassium chloride (CAS 7447-40-7), sodium phosphate dibasic (CAS 7784-85-6), and potassium phosphate monobasic (CAS 7778-77-0). Sucrose (Dominos sugar) was purchased at a local supermarket. Deionized water (DI) was used for all experiments.

System Characterization. The carbon working and counter electrodes were connected to the Zahner electrochemical workstation to evaluate the feasibility of using impedance spectroscopy to measure solution conductivity as a method for determining extent of sample concentration. The system was set to galvanostat mode with a typical two electrode setup. A 50 nA current setting and 50 nA amplitude were used for impedance measurements. The frequency was scanned from 1 Hz to 1 MHz during calibration and optimization, as shown in Figure S2 of the Supporting Information. Inline salt calibration data was obtained, and the optimal impedance measurement for calibration was observed at a frequency of 25 kHz. The calibration curves for sodium chloride and potassium chloride were linear between 0 and 100 mM concentrations, as shown in Figure S3. All impedance data for subsequent experiments were recorded at a frequency of 25 kHz. These initial experiments confirmed that impedance spectroscopy using carbon sensors could be used to determine sample concentration and to conduct salt diffusion studies through the membrane.

Copper electrodes have been shown to directly detect carbohydrates, including sucrose and glucose, using linear sweep voltammetry techniques.[54,55] Therefore, a copper electrode was integrated into the detection channel to be used as a working electrode and was connected to a CHI 1040C potentiostat. The carbon counter electrode and Ag/

DOI: 10.1021/acs.analchem.9b02163
Anal. Chem. 2019, 91, 7487−7494

AgCl reference electrode on the disposable sensor system were also connected to the potentiostat. Linear sweep voltammetry (LSV) was performed from 0 to 900 mV with a scan rate of 500 mV/s. The calibration of sugar concentration was performed by drawing samples through the inline monitoring assembly. Change in sugar concentration was determined by evaluating the change in current at a potential of 800 mV. The raw voltammetry scans are shown in Figure S4, with linear calibration data included in Figure S5. Test samples of 900–1000 μL volume were introduced into the system though the 1 mL sampling syringe. The venting syringe was used to release air while the sample was loaded into the setup.

Sucrose and potassium chloride, in varying concentrations up to the maximum solubility in water, were used as the draw solutions and were prepared at 200 mL volumes in a 200 mL glass beaker. Sucrose was prepared in concentrations of 1.7, 3.3, and 5.0 M (maximum solubility) in DI water. Potassium chloride was prepared in concentrations of 1.7, 3.3, 5.0, and 5.8 M (maximum solubility) in DI water. After the sample was filled into the system and ready for concentration, the membrane was submerged into the draw solution. Time dependent experiments were conducted by pulling 80 μL of sample into the sensor microchannel using the sampling syringe and by measuring the impedance for 10 s with the Zahner instrument. The CHI 1040C potentiostat would then record voltammetry data for 5 s. The 80 μL sample was then reintroduced back into the membrane. Separate experiments were run to determine water volume loss over time, and these required removal of all contents from the setup using the sampling syringe at 10 min intervals and then returning the sample after the volume was recorded.

RESULTS AND DISCUSSION

Draw Solution and Osmotic Pressure. Initial experiments were conducted to determine the rate of water flux (J_w) through the membrane over a 40 min period for the water–sucrose and water–KCl systems as a function of the osmotic driving force (Figure 2). The water flux was normalized to the 6.6 cm^2 surface area of the membrane. The membrane rejection of the two draw solutions was studied by using pure water as the test sample inside the membrane, while varying the concentration of the sucrose and KCl solutions outside the membrane. Equation 1 was referenced to correlate the water flux to membrane performance. The slope of the correlation in Figure 2 is the water permeability coefficient (K, eq 2), which was higher in the water–sucrose draw solution (K_s = 1.14 × 10^{-12} m s^{-1} Pa^{-1}) as compared to the water–KCl draw solution (K_{KCl} = 0.46 × 10^{-12} m s^{-1} Pa^{-1}). The values are similar to those reported values for cellulose membranes used in traditional NaCl forward osmosis systems that are typically operated with tangential flow (0.8–5.7 × 10^{-12} m s^{-1} Pa^{-1}).[56]

As described in eq 2, the osmotic reflection coefficient (σ) is considered 1 for systems where the membrane solute rejection is close to 100%. The assumption that σ = 1 was valid since the percent solute rejections of the membrane in the water–sucrose system (99.97%) and the water–KCl system (99.57%) are approximately 100%. As expected, higher water permeability coefficient and lower reverse solute flux produced higher water flux in the sucrose–water system, concluding that the membranes were able to reject sucrose to a greater extent than salt as the draw solution. This can be explained by the size of the sucrose molecules with a molecular weight of 342 g/mol as compared to potassium chloride, which has a molecular weight of 75 g/mol. The membrane rejection for the larger sucrose molecule also allows for a 3-fold increase in water flux when comparing sucrose to salt flux at a similar osmotic driving force. The membrane fouling mechanism of internal concentration polarization plays a key role, as investigated by Gray, for large scale desalination membranes.[57] The higher salt flux through the membrane significantly decreases the osmotic driving force, while the lower sucrose flux maintains the osmotic driving force, allowing for increased water flux. Using the maximum sucrose solubility in water, our system removed 600 μL of water in 40 min for a rate of 0.015 mL min^{-1}, starting from a 900 μL sample.

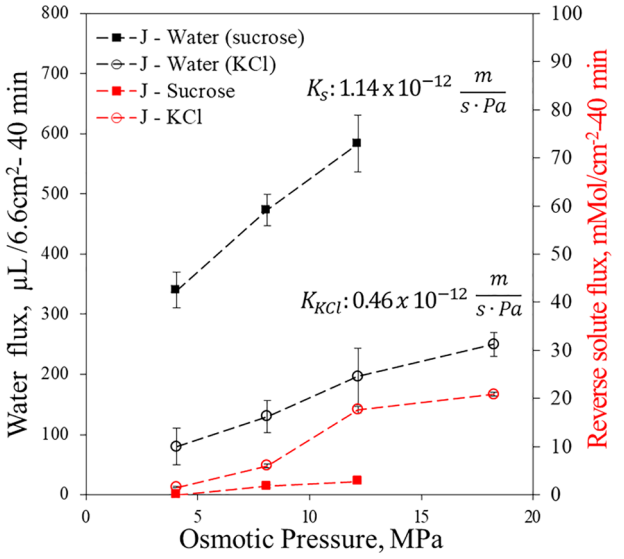

Figure 2. Osmotic pressure across the membrane was correlated to the water flux to acquire the resistance to solute diffusion coefficients for water–sucrose (K_s) and water–salt (K_{KCl}) systems. The osmotic pressure was controlled by varying the draw solute concentration. The water flux was normalized to the 6.6 cm^2 surface area of the membrane.

Temperature Impact. Bodily fluid sample temperature can vary depending on when the sample is analyzed. We evaluated the impact of temperature on water flux and draw solute reverse flux during sample concentration (Figure 3). The osmotic driving force was kept constant at 12 MPa, which correlated to sucrose at 5.0 M and salt at 2.5 M concentrations. At this osmotic driving force, water flux increased with temperature. Figure 3A shows a maximum water flux of 800 μL in 40 min or 0.02 mL min^{-1} at 40 °C in the water–sucrose system, while water flux leveled off for the water–KCl system. The decrease in flux for the water–sucrose system is caused by sucrose degrading to glucose and fructose at elevated temperatures.[58] These smaller sugars lead to internal concentration polarization (ICP), whereby increased reverse flux causes a significant reduction in water flux. Further investigation confirmed that increased temperatures led to higher reverse sucrose flux, as shown in Figure 3B.

pH Impact. Sample pH for bodily fluids can vary from 4.0–8.0. More basic pH was found to marginally decrease the water, sucrose, and salt flux (Figure 3C–E). This can be explained by cellulose ester membranes shrinking in basic conditions, as described by Kaur.[52] Figure 3C shows that the general water flux trend decreases by half at 10–60 min of operation due to ICP. This is a critical parameter for optimizing osmotic processes. Evaporative systems maintain

DOI: 10.1021/acs.analchem.9b02163
Anal. Chem. 2019, 91, 7487–7494

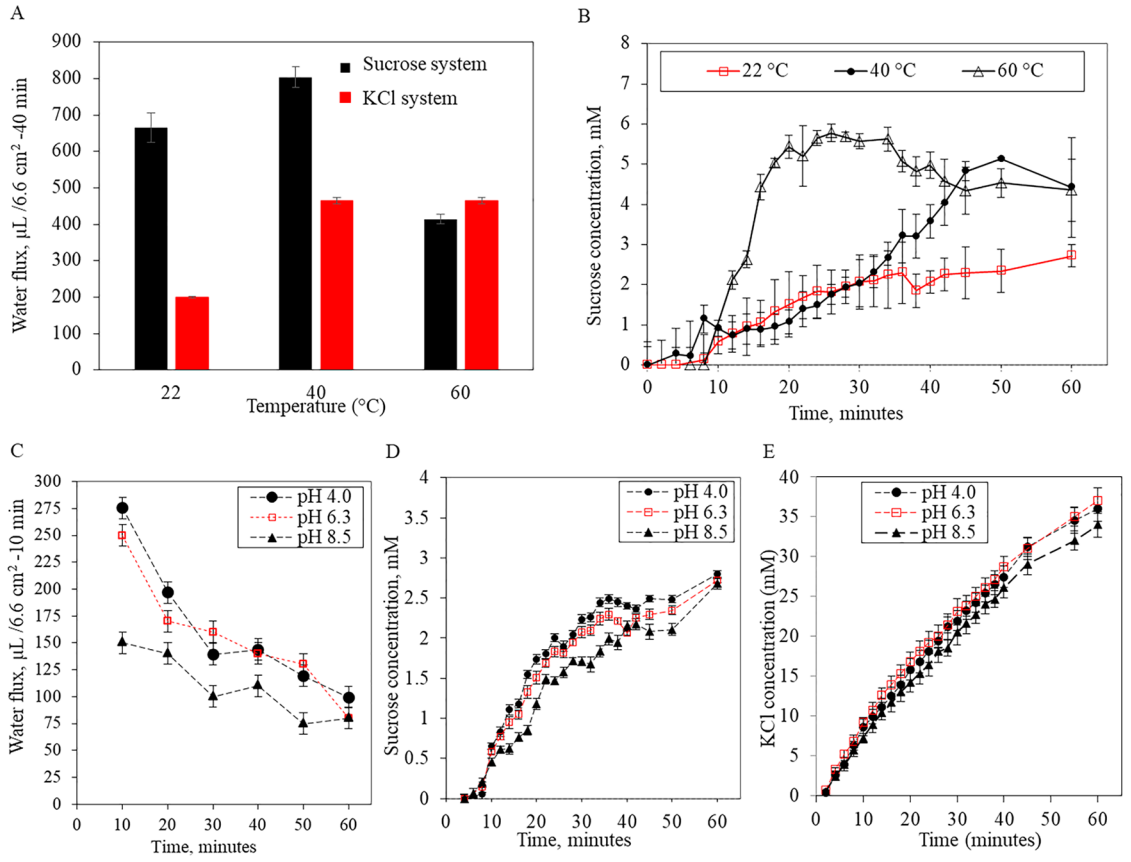

Figure 3. (A) Temperatures above 40 °C reduced water flux rates in the sugar system and remained similar in salt osmotic systems. (B) Significantly higher sucrose reverse flux was observed at 60 °C, which explains the observed reduction in water flux. (C) Impact of pH on water flux when sucrose is used as the draw solute. (D) Impact of pH on sucrose reverse flux. (E) Impact of pH on KCl osmotic system showed no pH impact to reverse solute flux, but the KCl system had higher solute flux as compared to the sucrose system.

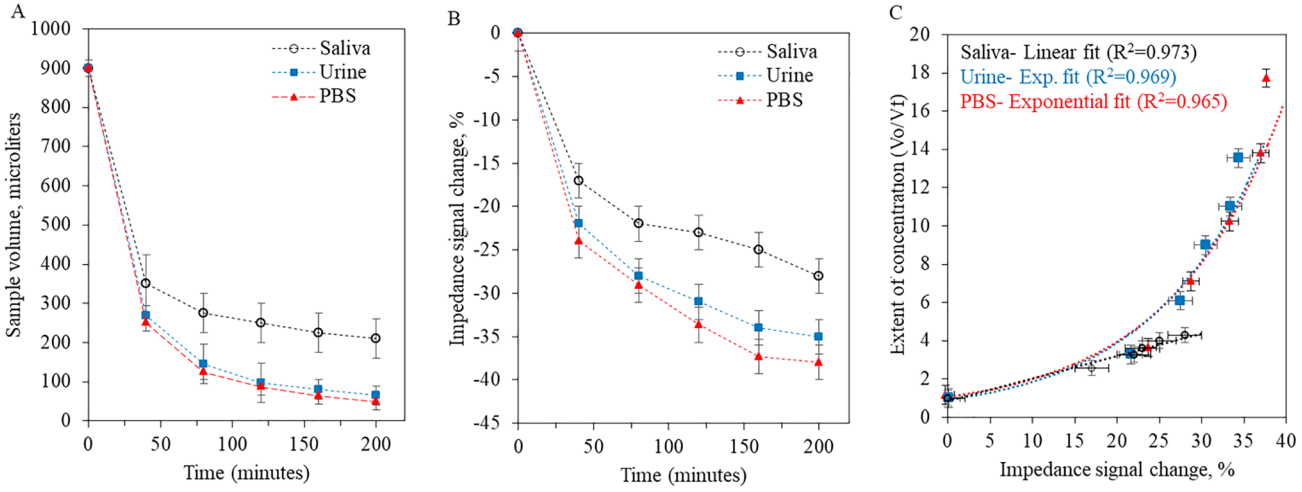

Figure 4. (A) Sample concentration measured by volume reduction compared to measurements using (B) impedance signal change shows PBS and urine have similar concentration profiles, while saliva concentrates to a lesser extent. (C) Impedance signal change correlated to the extent of concentration (V_f/V_0) shows an exponential fit to the experimental data for PBS and urine, while a linear trend fits the less concentrated saliva data.

a constant water removal rate by controlling the air flow rate above the gas−liquid interface. In this system, the initial water flux of 275 μL in 10 min or 0.025 mL min^{-1} can be maintained by removing the sample from one membrane into a newer membrane to maintain more constant water flux. Alternatively, optimization of membrane material, thickness, or porosity can enable constant water flux across the membrane for the duration of the concentration process.

A logarithmic relationship is observed between the duration of osmotic operation and the reverse solute flux for both sugar (Figure 3D) and salt (Figure 3E) systems, which can be modeled from the differential equation provided in eq 4 for solute concentrations. Membrane ICP created by the reverse

DOI: 10.1021/acs.analchem.9b02163
Anal. Chem. 2019, 91, 7487−7494

diffusion of solutes (KCl and sucrose) diminishes the water flux across the membrane. Therefore, a decreasing flux is observed for water over the 60 min concentration time, as shown in Figure 3C.

Bodily Fluid Samples. Stock solutions of 10 mM PBS were prepared to investigate the extent of sample concentration. In addition, urine and saliva samples from three healthy individuals were collected for testing of relevant biological samples.[59] Urine and saliva contain complex compounds that can lead to membrane fouling that may further diminish sample concentration using the osmotic system. The extent of sample concentration is the ratio between the initial to final sample volumes (V_0/V_f) and is used to quantify the concentration fold. The concentration fold was therefore measured using two methods. In the first method, a 1 mL syringe was used to determine water volume lost during concentration and is the gold standard used for determining concentration fold. The second method used the change in the impedance signal to measure the accumulated salt content in the sample as a result of concentration. As the sample concentrates, an increase in solute content decreases the impedance signal. The two characterization methods were performed for PBS, urine, and saliva samples (Figure 4).

Sucrose at maximum solubility (5.8 M) was used as the draw solution to concentrate all samples. Samples were run at room temperature to eliminate additional equipment, and pH was not adjusted. Sucrose at maximum solubility had a baseline pH value of 6.5. The use of sucrose for bodily fluid concentration was also advantageous because the reverse flux of sucrose did not interfere with impedance measurements. The experiments served to determine whether impedance data alone could be reliably used as an indicator of sample concentration in bodily fluids, while also determining to what extent bodily fluid samples could be concentrated in this system.

A decreasing trend was observed between the duration of osmotic operation and the change in sample volume, indicating that water was leaving the PBS, urine, and saliva samples (Figure 4A). In addition, the decrease in the impedance data confirmed solute enrichment (Figure 4B). The urine concentration profile was comparable to PBS concentration in both the volume-based and impedance-based measurements, indicating that the presence of additional compounds in the urine did not drastically impact the osmotic concentration. However, saliva samples showed a lower extent of sample concentration in both the volume-based and impedance-based measurements. The saliva data suggests the presence of membrane fouling compounds in the saliva as compared to urine and PBS samples.

The proposed impedance method was then correlated to the standard volume loss for all three samples, as presented in Figure 4C. An exponential correlation fit the experimental data best for PBS and was comparable for urine samples, indicating a 20-fold PBS sample concentration and a 15-fold urine concentration in 200 min. The saliva samples showed a linear fit between impedance and extent of sample concentration with a lower achievable concentration of 5-fold in 200 min. As previously described, the complex saliva samples contain compounds that negatively impact the ability to further concentrate the sample past 5-fold volume reduction. This data supports the use of impedance for monitoring of sample concentration in the osmotic system for bodily fluid samples.

Biomarker Concentration and Detection. The osmotic system was then coupled with electrochemical detection to detect a representative biomarker, pyocyanin, in bodily fluid samples. Pyocyanin is a redox active molecule produced by the *Pseudomonas aeruginosa* pathogen, whereby an electrochemical sensor can be utilized for detection. Pyocyanin has shown diagnostic promise in early identification of *P. aeruginosa* in multiple bodily fluid samples by using low-cost disposable carbon electrodes.[60,61] Relevant biological concentrations of pyocyanin are within the 0−10 μM range, while the current electrochemical limit of detection is approximately 0.5−1 μM. Electrochemical measurements of pyocyanin were performed using the disposable carbon electrodes in our system before and after osmotic concentration. A potentiostat (CH Instruments, CHI842C) was used to perform square-wave voltammetry (SWV) scans with an amplitude setting of 0.05 V and a frequency setting of 15 Hz in a potential window from −0.7 to 0.1 V against Ag/AgCl paste reference electrode. The height of the observed redox peaks from the SWV scans (Figure 5A) are due to the faradaic current, which can be correlated to pyocyanin concentration using a calibration curve.[62] A calibration was obtained by spiking known pyocyanin concentrations (0−10 μM range) into the test solutions and observing the faradaic current response at the detection potential range of −0.5 to 0.1 V. The first and

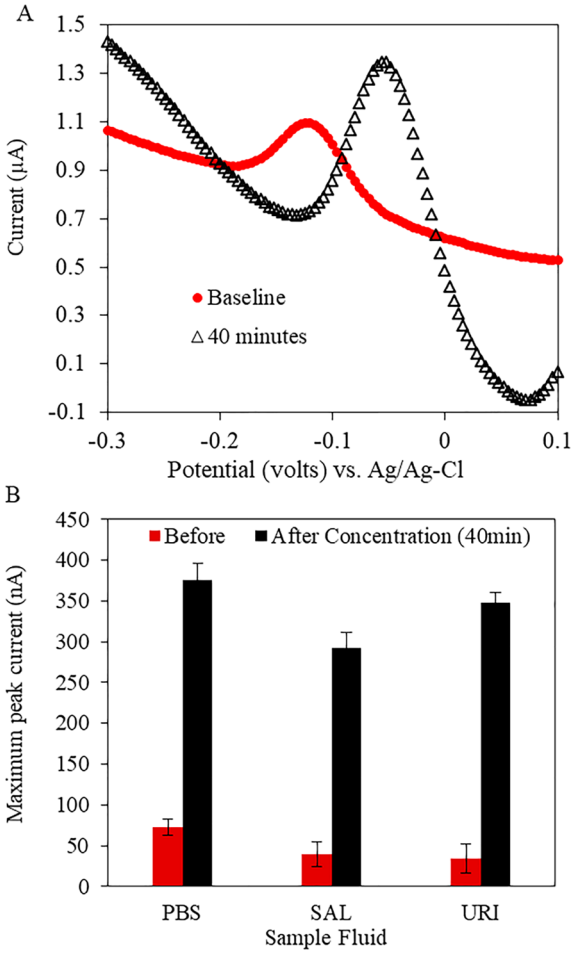

Figure 5. (A) SWV scan before and after 40 min of osmotic concentration for urine spiked with 1 μM pyocyanin. (B) PBS, saliva (SAL), and urine (URI) spiked with 1 μM pyocyanin showed the pyocyanin peak current increased by 350−400% after 40 min of forward osmosis.

DOI: 10.1021/acs.analchem.9b02163
Anal. Chem. 2019, 91, 7487−7494

second derivatives of the faradaic peak response were used to calculate half of the peak height at each tested pyocyanin concentration. The output of this calculation is referred to as the maximum peak current.

The three fluid samples (PBS, saliva, and urine) were each spiked with 1 μM pyocyanin. A 1 mL sample of each test fluid was then placed in the inside compartment of the osmotic system, while 5 M sucrose was placed as the draw solution to concentrate the samples for a duration of 40 min. Triplicate test samples were performed. Initial and final SWV scans were obtained to measure the pyocyanin redox peaks (Figure 5A). All three test fluids were found to yield a 350−400% peak signal increase after 40 min of concentration, as shown in Figure 5B, which corresponds to an up to 5-fold electrochemical signal increase. The fluid complexity did not have a considerable impact on the electrochemical signal amplification, as all three fluids showed similar results after being concentrated for 40 min.

CONCLUSIONS

We report a versatile integrated microfluidic design that allows for the concentration of bodily fluid samples without additional equipment. The system is capable of providing inline monitoring of microscale bodily fluid samples using cellulose ester membranes, copper electrodes, and disposable carbon electrodes. The system operation was characterized and optimized using sucrose as the draw solution. PBS, urine, and saliva samples were concentrated up to 20-fold (PBS), 15-fold (urine), or 5-fold (saliva) in less than 3 h. The system was then applied to the detection of pyocyanin to further show that the system can be used to increase the sensitivity of a target electroactive molecule in bodily fluids. We foresee integration of this simple method with multiple IVDPOCT systems to improve the limit of detection. This method can be further improved by moving samples into new membranes at set time intervals to minimize impact from ICP in the membrane. Alternatively, thinner membranes and different materials can be investigated to minimize the impact of ICP caused by reverse solute flux to maintain constant water flux.

ASSOCIATED CONTENT

Supporting Information

The Supporting Information is available free of charge on the ACS Publications website at DOI: 10.1021/acs.analchem.9b02163.

The detailed descriptions of the fabricated system and calibration data for sample solutes using impedance spectroscopy and sugar using copper electrode linear sweep voltammetry (PDF)

AUTHOR INFORMATION

Corresponding Author

*E-mail: e.goluch@northeastern.edu.

ORCID

Edgar D. Goluch: 0000-0001-9319-8906

Author Contributions

M.K.K. and E.D.G. designed the experiments. M.K.K. and R.L. performed the experiments and data analysis. M.K.K. and E.D.G. wrote and edited the manuscript.

Notes

The authors declare the following competing financial interest(s): E.D.G. has a financial interest in a company that is commercializing part of the described technology.

ACKNOWLEDGMENTS

This work was supported, in part, by award #1740961 from the National Science Foundation. R.L. thanks Northeastern University for providing an Undergraduate Research Award.

ABBREVIATIONS

Ag/AgCl	silver/silver chloride
ICP	internal concentration polarization
IVPODCT	in vitro diagnostic point of care testing
MWCO	molecular weight cutoff
PDMS	polydimethylsiloxane
SEM	scanning electron microscope
HPLC-MS	high-performance liquid chromatography mass spectrometry
PCR	polymerase chain reaction
ELISA	enzyme-linked immunosorbent assay
LOD	limit of detection

REFERENCES

(1) Nováková, L.; Vlčková, H. *Anal. Chim. Acta* **2009**, *656*, 8−35.
(2) Esser, D.; Alvarez-Llamas, G.; de Vries, M.; Weening, D.; Vonk, R. J.; Roelofsen, H. *Biomarker Insights* **2008**, *3* (3), 25−37.
(3) Yin, R.; Mo, J.; Lu, M.; Wang, H. *Anal. Chem.* **2015**, *87* (3), 1846−1852.
(4) Wilson, I. D.; Plumb, R.; Granger, J.; Major, H.; Williams, R.; Lenz, E. M. *J. Chromatogr. B: Anal. Technol. Biomed. Life Sci.* **2005**, *817*, 67−76.
(5) Nally, J. E.; Mullen, W.; Callanan, J. J.; Mischak, H.; Albalat, A. *Proteomics: Clin. Appl.* **2015**, *9*, 543.
(6) Fang, X.; Balgley, B. M.; Lee, C. S. *Electrophoresis* **2009**, *30* (23), 3998−4007.
(7) Bakry, R.; Huck, C. W.; Najam-Ul-Haq, M.; Rainer, M.; Bonn, G. K. *J. Sep. Sci.* **2007**, *30* (2), 192−201.
(8) Jeun, M.; Park, S.; Lee, H.; Lee, K. H. *Int. J. Nanomed.* **2016**, *11*, 5497−5503.
(9) Lee, H.; Yoon, T.-J.; Figueiredo, J.-L.; Swirski, F. K.; Weissleder, R. *Proc. Natl. Acad. Sci. U. S. A.* **2009**, *106* (30), 12459−12464.
(10) Lee, H.; Yoon, T.-J.; Weissleder, R. *Angew. Chem., Int. Ed.* **2009**, *48*, 5657−5660.
(11) Weinstein, E. A.; Ordonez, A. A.; DeMarco, V. P.; Murawski, A. M.; Pokkali, S.; MacDonald, E. M.; Klunk, M.; Mease, R. C.; Pomper, M. G.; Jain, S. K. *Sci. Transl. Med.* **2014**, *6* (259), 259ra146−259ra146.
(12) Rissin, D. M.; Kan, C. W.; Campbell, T. G.; Howes, S. C.; Fournier, D. R.; Song, L.; Piech, T.; Patel, P. P.; Chang, L.; Rivnak, A. J. *Nat. Biotechnol.* **2010**, *28* (6), 595−599.
(13) De La Rica, R.; Stevens, M. M. *Nat. Nanotechnol.* **2012**, *7* (12), 821−824.
(14) Niemz, A.; Ferguson, T. M.; Boyle, D. S. *Trends Biotechnol.* **2011**, *29*, 240−250.
(15) Song, Y.; Huang, Y. Y.; Liu, X.; Zhang, X.; Ferrari, M.; Qin, L. *Trends Biotechnol.* **2014**, *32*, 132−139.
(16) Zarei, M. *Biosens. Bioelectron.* **2017**, *98*, 494−506.
(17) Loonen, A. J. M.; Schuurman, R.; Van Den Brule, A. J. C. *Expert Rev. Mol. Diagn.* **2012**, *12*, 17−19.
(18) Griss, R.; Schena, A.; Reymond, L.; Patiny, L.; Werner, D.; Tinberg, C. E.; Baker, D.; Johnsson, K. *Nat. Chem. Biol.* **2014**, *10* (7), 598−603.
(19) Thomas, D. J.; Tehrani, Z. *Point Care.* **2016**, *15* (2), 61−71.
(20) Crp, P. *Drug Ther. Bull.* **2016**, *54* (10), 117−120.

DOI: 10.1021/acs.analchem.9b02163
Anal. Chem. 2019, 91, 7487−7494

(21) Gubala, V.; Harris, L. F.; Ricco, A. J.; Tan, M. X.; Williams, D. E. *Anal. Chem.* **2012**, *84*, 487−515.
(22) Su, J.; Xu, J.; Chen, Y.; Xiang, Y.; Yuan, R.; Chai, Y. *Chem. Commun.* **2012**, *48* (55), 6909.
(23) Su, W.; Gao, X.; Jiang, L.; Qin, J. *Journal of Chromatography A* **2015**, *1377*, 13−26.
(24) Vasan, A. S. S.; Doraiswami, R.; Mahadeo, D. M.; Huang, Y.; Pecht, M. *Front. Biosci., Scholar Ed.* **2013**, *S5*, 39−71.
(25) Lee-Lewandrowski, E.; Lewandrowski, K. *Clin. Lab. Med.* **2001**, *21* (2), 217−240.
(26) Musiani, M.; Venturoli, S.; Gallinella, G.; Zerbini, M. *Nat. Protoc.* **2007**, *2* (10), 2502−2510.
(27) Pamme, N. *Lab Chip* **2007**, *7* (12), 1644.
(28) Tang, R.; Yang, H.; Choi, J. R.; Gong, Y.; Hu, J.; Feng, S.; Pingguan-Murphy, B.; Mei, Q.; Xu, F. *Talanta* **2016**, *152*, 269−276.
(29) Park, S.; Zhang, Y.; Wang, T. H.; Yang, S. *Lab Chip* **2011**, *11* (17), 2893−2900.
(30) Lynn, N. S.; Šípová, H.; Adam, P.; Homola, J. *Lab Chip* **2013**, *13* (7), 1413.
(31) Rahman, M. M.; Ahammad, A. J. S.; Jin, J. H.; Ahn, S. J.; Lee, J. J. *Sensors* **2010**, *10* (5), 4855−4886.
(32) Shanmugam, N. R.; Muthukumar, S.; Prasad, S. *Sci. Rep.* **2016**, *6* (1), 33423.
(33) Vergauwen, G.; Dhondt, B.; Van Deun, J.; De Smedt, E.; Berx, G.; Timmerman, E.; Gevaert, K.; Miinalainen, I.; Cocquyt, V.; Braems, G. *Sci. Rep.* **2017**, *7* (1), 2704 DOI: 10.1038/s41598-017-02599-y.
(34) Ho, N. T.; Fan, A.; Klapperich, C. M.; Cabodi, M. *Proceedings of the Annual International Conference of the IEEE Engineering in Medicine and Biology Society, EMBS.* **2012**, 2396−2399.
(35) Tseng, W. Y.; Van Dam, R. M. *Lab Chip* **2014**, *14* (13), 2293−2302.
(36) Sander, L. C. *NIST JRES* **2017**, *122* (11), 6028.
(37) Corstjens, P. L. A. M.; Nyakundi, R. K.; de Dood, C. J.; Kariuki, T. M.; Ochola, E. A.; Karanja, D. M. S.; Mwinzi, P. N. M.; van Dam, G. J. *Parasites Vectors* **2015**, *8*, 241.
(38) Abeysena, I.; Darrington, R. *Am. Lab. Technol.* **2013**, 131586.
(39) Guy, J. L.; Serveau, M. Process for Concentrating Specimens by Evaporation of the Solvent with a Centrifugal Evaporator-Concentrator. United States Patent 5084133, 1992.
(40) Wong, S. Y.; Cabodi, M.; Rolland, J.; Klapperich, C. M. *Anal. Chem.* **2014**, *86* (24), 11981−11985.
(41) Sharma, N. R.; Lukyanov, A.; Bardell, R. L.; Seifried, L.; Shen, M. *Proc. SPIE* **2008**, *6886*, 68860R−9.
(42) Timmer, B. H.; Van Delft, K. M.; Olthuis, W.; Bergveld, P.; Van den Berg, A. *Sens. Actuators, B* **2003**, *91* (1−3), 342−346.
(43) Xie, X.; Bahnemann, J.; Wang, S.; Yang, Y.; Hoffmann, M. R. *Sci. Rep.* **2016**, *6*, 1−8.
(44) Walker, G. M.; Beebe, D. J. *Lab Chip* **2002**, *2* (2), 57−61.
(45) Kimani, M. K.; Mwangi, J.; Goluch, E. D. *J. Anal. Test.* **2019**, 1 DOI: 10.1007/s41664-019-00096-x.
(46) Blandin, G.; Vervoort, H.; Le-Clech, P.; Verliefde, A. R. D. *J. Water Process Eng.* **2016**, *9*, 161−169.
(47) Kwon, S. J.; Park, S. H.; Park, M. S.; Lee, J. S.; Lee, J. H. *J. Membr. Sci.* **2017**, *544* (June), 213−220.
(48) Butler, E.; Silva, A.; Horton, K.; Rom, Z.; Chwatko, M.; Havasov, A.; McCutcheon, J. R. *Desalination* **2013**, *312*, 23−30.
(49) Akther, N.; Sodiq, A.; Giwa, A.; Daer, S.; Arafat, H. A.; Hasan, S. W. *Chem. Eng. J.* **2015**, *281*, 502−522.
(50) Cath, T. Y.; Childress, A. E.; Elimelech, M. *J. Membr. Sci.* **2006**, *281*, 70−87.
(51) Phillip, W. A.; Yong, J. S.; Elimelech, M. *Environ. Sci. Technol.* **2010**, *44* (13), 5170−5176.
(52) Kaur, H.; Bulasara, V. K.; Gupta, R. K. *Carbohydr. Polym.* **2018**, *195* (May), 613−621.
(53) Ong, R. C.; Chung, T. S.; de Wit, J. S.; Helmer, B. J. *J. Membr. Sci.* **2015**, *473*, 63−71.
(54) Prabhu, S. V.; Baldwin, R. P. *Anal. Chem.* **1989**, *61* (20), 2258−2263.
(55) Ye, J.; Baldwin, R. P. *J. Chromatogr. A* **1994**, *687* (1), 141−148.
(56) Lutchmiah, K.; Verliefde, A. R. D.; Roest, K.; Rietveld, L. C.; Cornelissen, E. R. *Water Res.* **2014**, *58*, 179.
(57) Gray, G. T.; McCutcheon, J. R.; Elimelech, M. *Desalination* **2006**, *197* (1−3), 1−8.
(58) Tombari, E.; Salvetti, G.; Ferrari, C.; Johari, G. P. *J. Phys. Chem. B* **2007**, *111* (3), 496−501.
(59) Alatraktchi, F. A.; Andersen, S. B.; Johansen, H. K.; Molin, S.; Svendsen, W. E. *Sensors* **2016**, *16* (3), 408.
(60) Santiveri, C. R.; Sismaet, H. J.; Kimani, M.; Goluch, E. D. *Chemistry Select.* **2018**, *3* (11), 2926−2930.
(61) Sismaet, H. J.; Banerjee, A.; McNish, S.; Choi, Y.; Torralba, M.; Lucas, S.; Chan, A.; Shanmugam, V. K.; Goluch, E. D. *Wound Repair Regen.* **2016**, *24* (2), 366−372.
(62) Webster, T. A.; Sismaet, H. J.; Conte, J. L.; Chan, I.-P. J.; Goluch, E. D. *Biosens. Bioelectron.* **2014**, *60*, 265−270.

DOI: 10.1021/acs.analchem.9b02163
Anal. Chem. 2019, 91, 7487−7494